

**ANALYSIS AND DESIGN OF DUAL BAND HIGH DIRECTIVITY EBG RESONATOR ANTENNA USING SQUARE LOOP FSS AS SUPERSTRATE LAYER**

**A. Pirhadi**

Department of Electrical Engineering  
Tarbiat Modares University (TMU)  
Tehran, Iran

**F. Keshmiri**

Iran University of Science and Technology (IUST)  
Tehran, Iran

**M. Hakkak**

Department of Electrical Engineering  
Tarbiat Modares University (TMU)  
Tehran, Iran

**M. Tayarani**

Iran University of Science and Technology (IUST)  
Tehran, Iran

**Abstract**—A superstrate layer is used to enhance the directivity of the small radiation sources such as Microstrip Patch Antennas. In this paper, we use square loop frequency selective surface (SL-FSS) configuration to design the superstrate layer. To compact the structure, we propose a new single layer square loop FSS configuration that operates in two frequency bands such as multi-layer SL-FSS. Simulation results are shown to have good agreement with experimental results.

## 1. INTRODUCTION

Electromagnetic Bandgap (EBG) structures are periodic structures that are composed of dielectric, metal or metallo-dielectric materials. These structures prevent wave propagation in special directions and frequencies. Therefore, they can be used as spatial and frequency filters [2]. One of the applications of 2-D EBG is using them as superstrate layers to enhance the directivity of small radiation sources such as Microstrip Patch Antennas. Due to the 2-D periodicity of FSS structures they can be used as 2-D EBG superstrates in high directive EBG resonator antennas. Various types of FSS elements are used in this configuration such as strip, patch and cross strip [10]. In this paper, we use a special composition of square loop FSS structures in which we can design dual band and compact high directive antenna. The advantages of using square loop elements for designing FSS compositions are their symmetrical geometry making them suitable to obtain horizontal and vertical polarization, producing several resonance frequencies by combination of different loop sizes in each cell, and their small size compared with other kinds of FSS elements such as patch elements [11]. All simulations have been done using Ansoft Designer software based on the Method of Moment (MOM).

## 2. DESIGN OF THE FSS SUPERSTRATE LAYER

The original configuration treated here, includes a printed patch antenna and superstrate layers above it (Figure 1(a)). The superstrate layer can enhance both directivity and bandwidth of the patch antenna [1]. The superstrate layer and the ground plane, shown in Figure 1(a), when excited with a plane wave make a resonator in  $Z$  direction. Therefore, the resonance frequencies of the structure that are called defect frequencies are related to superstrate layers and their distances to ground plane. Due to the defect frequencies, the directivity of primary radiation source embedded in the structure enhanced considerably. Therefore, suitable design of FSS structure, as superstrate layer is the most important part of high directive antenna design.

### 2.1. The Geometry of the Superstrate Structure

The usual method to investigate the characteristics of the structure is examining both superstrate layer and its image on the ground plane using image theory [3]. This is done by eliminating the ground

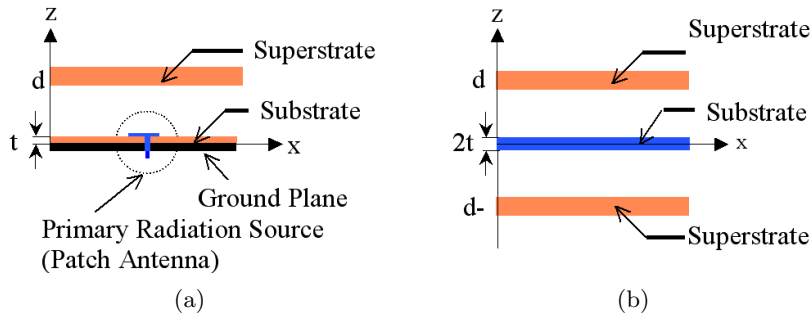


**Figure 1.** (a) Superstrate layer above a printed patch antenna at  $z = d$  (b) The ground plane is replaced by the image of superstrate layer at  $z = -d$ .

plane and adding a similar superstrate layer at  $z = -d$ , as shown in Figure 1(b). This configuration is a 2-D EBG structure that is infinitely periodic in  $X$ ,  $Y$  directions and finite in  $z$  direction. Therefore, its properties are characterized using periodic boundary condition for each unit cell.

In this case, the shape and separation of the FSS elements affects the transmission and reflection coefficients of the whole structure and controls the defect frequencies.

Figure 2 shows one cell of FSS layer consisting of infinite numbers of loops with  $P = 5.06$  mm, where  $P$  is the periodicity of the unit cell. The Loops have inner and outer length of  $a_i$  and  $a_o$ . Depending on the number of operating frequencies, the superstrate above the patch antenna can have one layer (Figure 2(a)) or more (Figure 2(b)).

## 2.2. Method of Analysis

To obtain the transmission and reflection coefficients of the structure in Figure 2, it is illuminated from the bottom in the  $z$  direction by a linear polarization plane wave. We see that FSS element characteristics (dimensions of square loop and periodicity) and the distance between the FSS layers control the resonance frequencies. To study the characteristics of the superstrate layer, five categories of unit cells with different FSS configurations are studied which are: 1- One-layer superstrate with one-sided square loop elements, 2- Two-layer FSS with one-sided square loop elements, 3- Four-layer FSS with one-sided square loop elements, 4- Two-layer FSS with double one-sided square loop elements, and 5- Two-layer FSS with two-sided square loop elements.

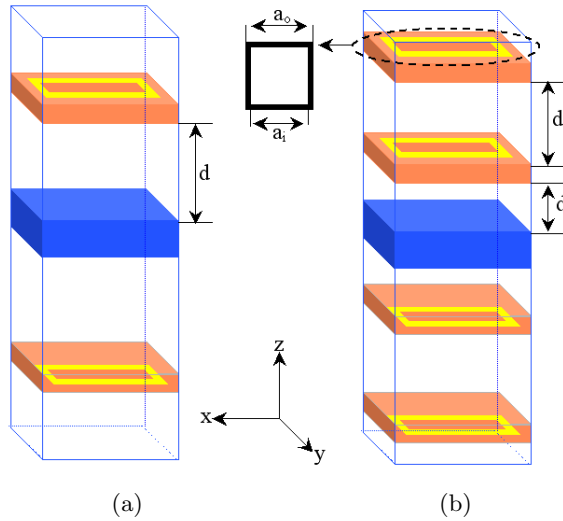


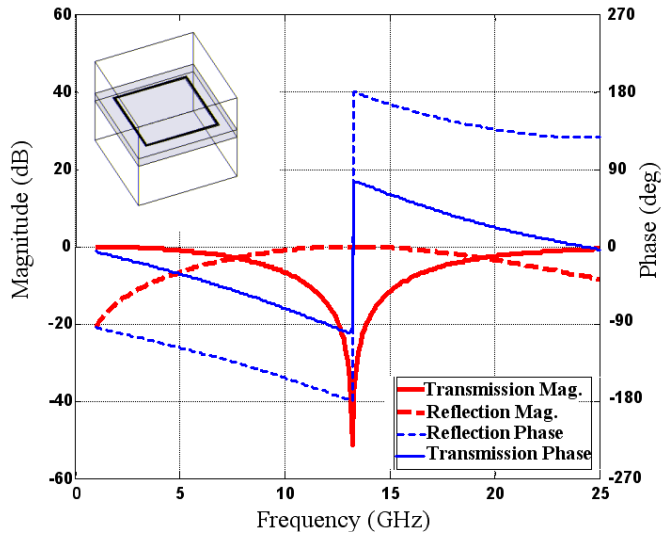
**Figure 2.** (a) Unit cell of the two-layer FSS with square loop elements. (b) Geometry of the square loop elements and the unit cell with four-layer FSS.

The first configuration determines the reflection and transmission coefficients of each superstrate layer, providing a base for the study of other combinations. The second and third ones are used for single- and dual-band superstrate designs, respectively. The fourth and fifth ones describe compact superstrates that operate in two or more frequency bands.

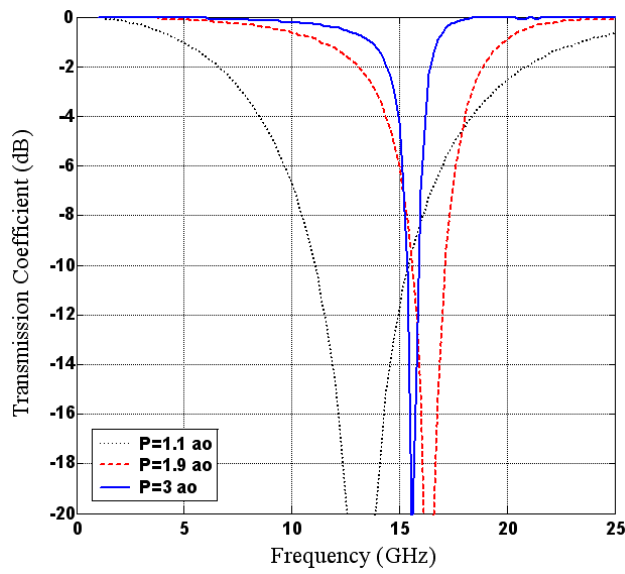
### 2.2.1. One-layer FSS with One-Sided Square Loop Elements

The One-layer FSS consists of square loop elements backed by the related dielectric as shown in Figure 3(a). At resonant frequency ( $f_0 \approx 14$  GHz), we have total reflection and at other frequencies it has partially reflection and transmission coefficients. The bandwidth (BW) of the structure is defined as frequency region in which we have total reflection or near total reflection. In the following, we examine the effects of the periodicity on the magnitude of the reflection and transmission coefficients and its effect on the bandwidth of the structure. If the spacing between FSS elements increases uniformly, the quality factor ( $1/\text{BW}$ ) increases as shown in Figure 3(b).

The transmission characteristic of the unit cell as a function of  $P$  is shown in Figure 4, for  $a_i = 4.2$  mm,  $a_o = 4.6$  mm. We observe that the resonance frequency increases from 9 GHz to 16.5 GHz as the



(a)



(b)

**Figure 3.** (a) Transmission and reflection coefficient (magnitude and phase) of a one-layer FSS with square loop elements, versus frequency ( $a_o = 4.6$ ,  $a_i = 4.2$ ,  $P = 1.1a_o$ ) (b) Transmission coefficients for different periodicity of FSS elements.

periodicity  $P$  is increased from  $a_o$  ( $= 4.6$  mm) to  $1.9a_o$  ( $= 8.74$  mm) and then decreases from 16.5 GHz to 12.5 GHz as  $P$  is increased from  $1.9a_o$  ( $= 8.74$  mm) to  $5a_o$  ( $= 23$  mm).

To decrease the total area of the structure we should choose the proper periodicity of the elements in the  $x$ - $y$  plane. As shown in Figure 4, if the FSS elements lie close to each other ( $P \approx a_o$ ), the structure would be the smallest one. An important factor that must be noticed is that though closely spacing of FSS elements results in area and frequency reduction, it results in a bad Q-factor. Therefore, we have to be careful in choosing the array element size. With respect to the total size of the FSS in the  $XY$  plane and quality factor of the loop resonance, we choose the periodicity of the FSS elements equal to  $1.1a_o = 5.06$  mm.

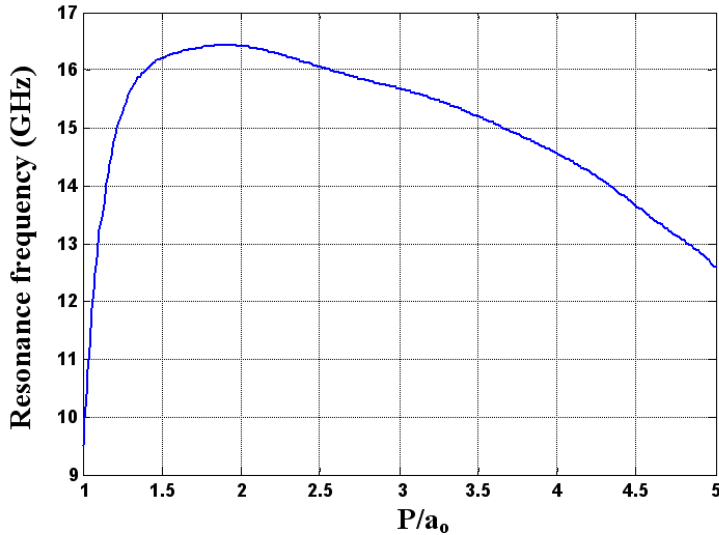
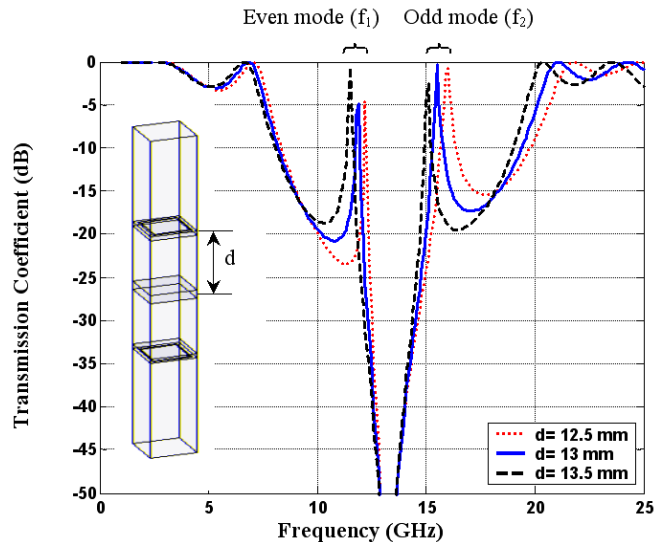


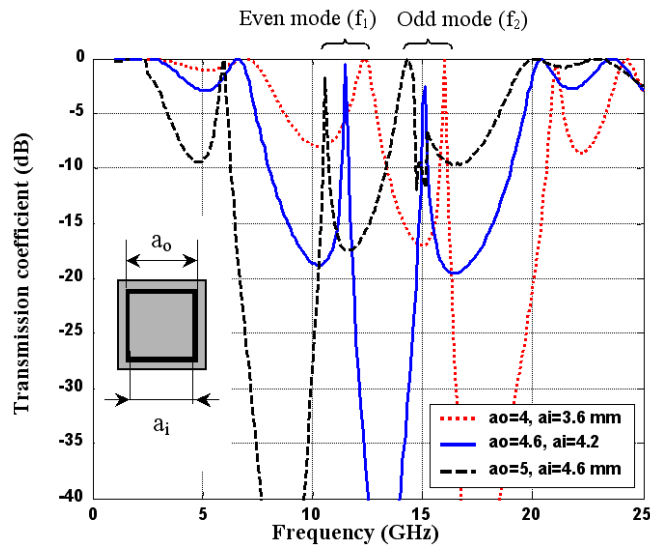
**Figure 4.** Resonance frequency of one-layer FSS as a function of FSS elements Periodicity ( $P$ ), for  $a_i = 4.2$  mm,  $a_o = 4.6$  mm.

### 2.2.2. Two-layer FSS with One-sided Square Loop Elements

Since a single-layer FSS yields one resonance frequency  $f_0$  with narrow bandgap (Figure 3(b)), we stack another FSS layer above it. By adjusting the distance between the layers (defect length  $d$ ) to about  $\lambda_o/4$ , it is possible to achieve a wider bandgap. Also changing this parameter leads to producing resonance frequencies in the bandgap region, which are called defect frequencies. These characteristics are shown in Figure 5(a). The defect frequencies  $f_1, f_2$  would be decreased



(a)



(b)

**Figure 5.** Transmission coefficient of the two-layer FSS versus frequency ( $P = 5.06$  mm) (a) for different defect lengths  $d$ . ( $a_o = 4.6$ ,  $a_i = 4.2$  mm) (b) for different loop sizes ( $d = 13.5$  mm).

by increasing  $d$ . Therefore, the defect length ( $d$ ) easily controls the defect frequencies.

Note that, since varying  $d$  would move both defect frequencies, we should adjust the  $f_0$  by the geometry of the FSS elements, too. The effect of varying  $f_0$  on  $f_1, f_2$  is shown in Figure 5(b). It is noticed that  $f_0$  can shift  $f_1$  and  $f_2$ , thus changing their quality factor and sometimes eliminates either  $f_1$  or  $f_2$ . It is seen from this figure that the resonance frequency of the loop ( $f_0$ ) can be smaller than  $f_1$  (dash), greater than  $f_2$  (dot) or located between  $f_1$  and  $f_2$  (solid). In the first case, the quality factor of  $f_2$  decrease that is not apposite here. Similarly in the second one the quality factor of  $f_1$  is reduced. If  $f_0$  is located between  $f_1$  and  $f_2$ , it leads to two high- $Q$  defect frequencies at  $f_1$  and  $f_2$ .

The variations of the defect modes versus  $f_0$  for different modes are shown in Figure 6. One of the most important advantages of using the FSS layer in designing the superstrate layer is its ability to obtain suitable reflection coefficient at the operating frequency. This ability helps us to obtain the desired quality factor at the resonance frequency.

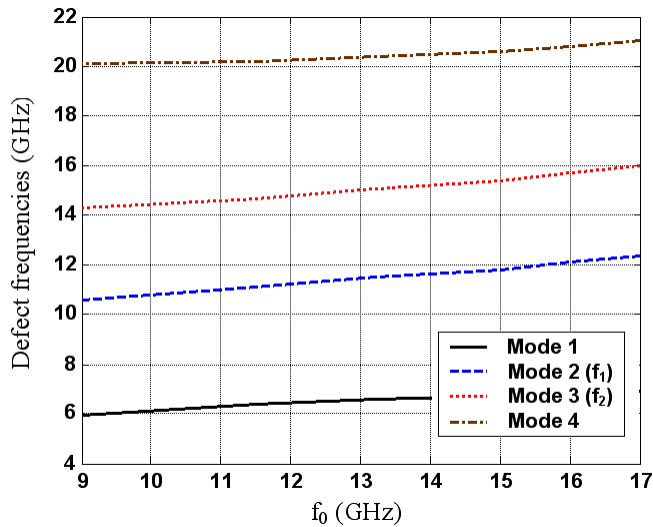


**Figure 6.** Variation of the defect modes versus  $f_0$  for different modes.

The single-layer FSS superstrate, which is modeled with two-layer FSS in an EBG unit cell, enhances the directivity of an embedded radiation source only at even modes. This is due to the zero tangential electric fields on the symmetrical plane (Ground Plane) [1–4]. Figure 7 shows the electric field distributions for different defect modes (mode 1-4). As shown, only in modes 2 and 4 there are zero tangential electric



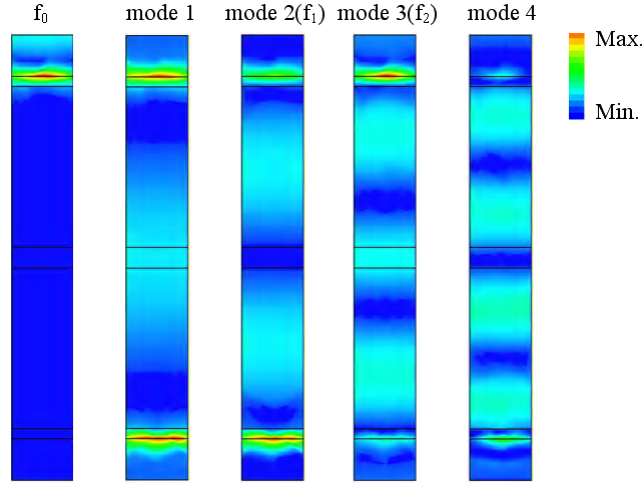


**Figure 7.** Electric field distributions of different defect modes (1-4).

fields. Also, because of the low quality factor of mode 4, it cannot be used to direct the primary radiation source.

### 2.2.3. Four-layer FSS with One-sided Square Loop Elements

A two-layer superstrate (four FSS layers in a unit cell) is used to achieve directivity enhancement in a two-frequency band. This structure (Figure 8(a)) resonates at three different frequencies  $f_1$ ,  $f_2$ , and  $f_3$  in which, insertion of the upper FSS layer creates two adjustable high  $Q$  defect frequencies in a band gap. As mentioned in the previous section, only even defect modes ( $f_1$ ,  $f_2$ ) can be used to achieve high directivity.

In this Figure,  $f_1$  and  $f_2$  are the even defect modes that can be controlled by  $d$  and  $d'$ , respectively. The resonance frequencies of layers are related to FSS characteristic and are independent from the defect lengths ( $d$ ,  $d'$ ).  $f_2$  would be equal to 14 and 12.15 GHz, if we choose  $d'$  equal 10.25 and 12.75 mm. Also,  $f_2$  can be disappeared in resonance of the loops, if  $d'$  equals 11.25 mm.

The four-layer FSS creates a band gap of 81.48% as compared with that of the one-layer and two-layer FSS, i.e., 3.25% and 15.85%, respectively (Table 1). Note that the bandwidth is measured without any defect frequency and this is possible by adjusting the defect lengths  $d$ ,  $d'$  to about  $\lambda/4$ .

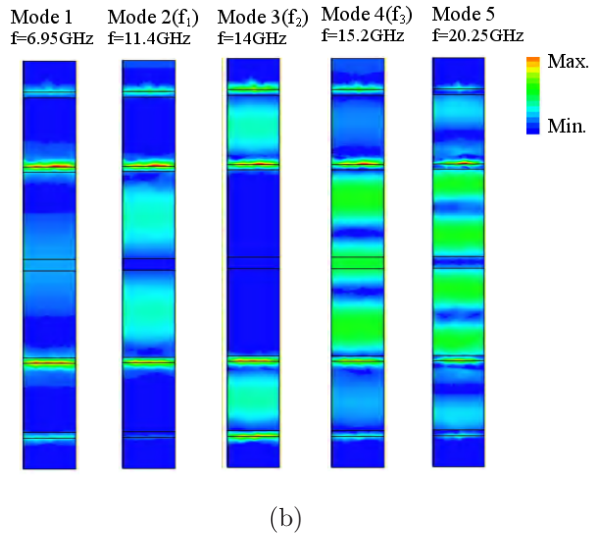
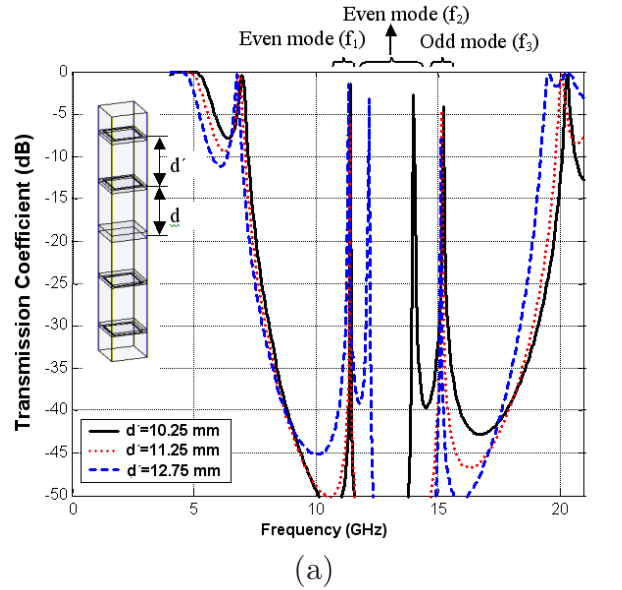


**Figure 8.** (a) Transmission coefficient of the four-layer FSS versus frequency ( $P = 5.06$ ,  $d = 13.5$  mm) for different  $d'$ . ( $a_o = a'_o = 4.6$  mm,  $a_i = a'_i = 4.2$  mm) (b) Electric field distribution for odd and even modes.

**Table 1.** Comparison between the bandgaps of different FSS types.

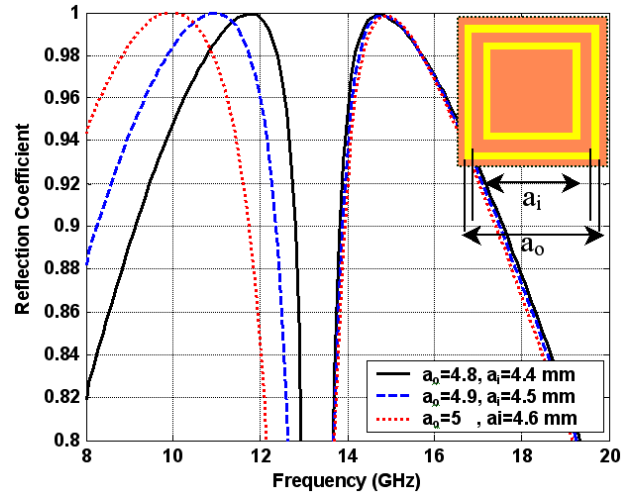
| The type of geometrical construction of superstrate                | Bandwidth of the gap without any defect (below -30 dB) |
|--|--|
| <i>One Layer FSS with One-sided Square Loop (Figure 3)</i>         | % 3.2  |
| <i>Two Layer FSS with One-sided Square Loop (Figure 5)</i>         | % 15.8   |
| <i>Four Layer FSS with One-sided Square Loop (Figure 8)</i>        | % 81.5   |
| <i>Two Layer FSS with Double One-sided Square Loop (Figure 10)</i> | % 46.5   |
| <i>Two Layer FSS with Double Two-sided Square Loop (Figure 13)</i> | % 62.9   |

#### 2.2.4. One-layer FSS with Double One-sided Square Loop Elements

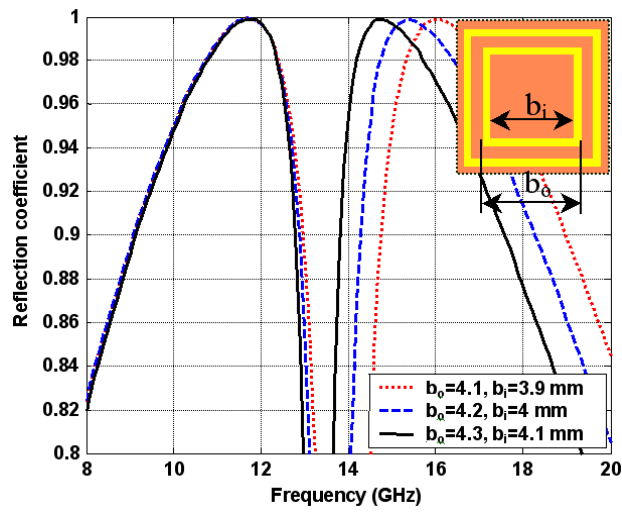
Another way to make two defect frequencies in a wide band gap is to use a double one-sided square loop above a patch antenna [2]. The high  $Q$  defect modes of two layer FSS with this element are excited near the resonance frequencies of single layer FSS, in which full reflection occurs. In other words, we should design one layer FSS by double one-sided elements with almost perfect reflections in two separate frequencies where the first one (second one) can be tuned by  $a_o$  and  $a_i$  ( $b_o$  and  $b_i$ ), as shown in Figures 9(a) and (b).

Simulations show that the two resonance frequencies are almost independent of each other. Resonance frequencies of Figure 9 can be neared to each other by decreasing  $a_o$  and  $a_i$  (or increasing  $b_o$  and  $b_i$ ). But, the fabrication process limits us to extremely close the loop lines to obtain the wanted resonance frequencies. Complete reflection can be seen at 11.85 GHz and 14.65 GHz for  $a_o = 4.8$  mm,  $a_i = 4.4$  mm,  $b_o = 4.3$  mm,  $b_i = 4.1$  mm (solid lines in Figure 9). Similar to previous sections, the transmission coefficient of two layers of this type of SL-FSS, with different defect lengths,  $d$ , are shown in Figure 10.

By adjusting the FSS layer distance the even frequencies move to the desired frequencies. To identify the even modes we show the field distribution of some important modes in Figure 11 where the feasible even modes are created at 10.5 GHz and 13.9 GHz, being obtained by defect length  $d = 43$  mm. The most disadvantage of this configuration is its large defect length compared to previous configurations.



(a)



(b)

**Figure 9.** Reflection coefficient of the one-layer FSS with double one-sided square loops versus frequency ( $P = 5.175$  mm) (a) for different  $a$  ( $b_o = 4.3, b_i = 4.1$  mm) (b) for different  $b$  ( $a_o = 4.8, a_i = 4.4$  mm).

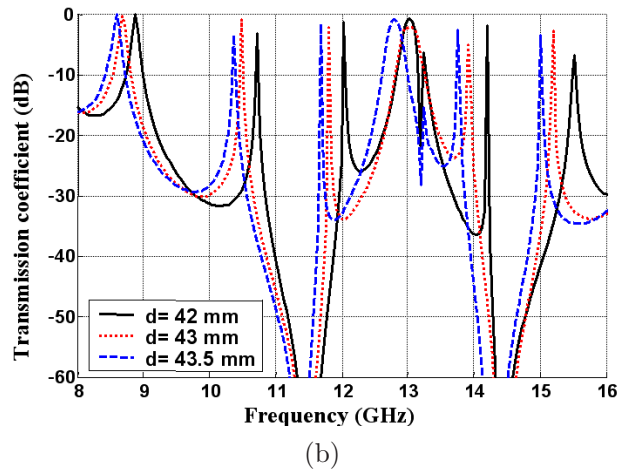
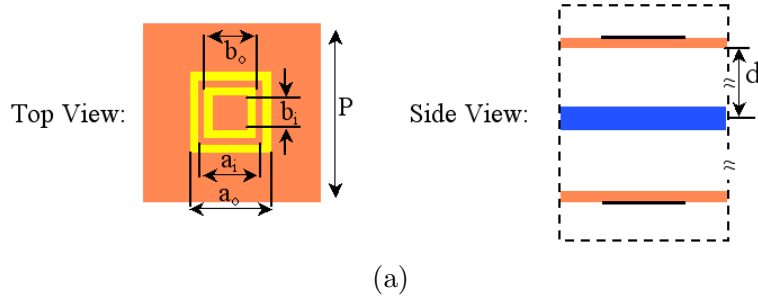


**Figure 10.** (a) Two-layer FSS with double one-sided square loop elements (b) Transmission coefficient versus frequency. ( $P = 5.175$ ,  $a_o = 4.8$ ,  $a_i = 4.4$ ,  $b_o = 4.3$ ,  $b_i = 4.1$  mm).

*2.2.5. Two-layer FSS with Two-sided Square Loop Elements*

By printing the second loop on the other side of the layer, we have more ability to control the resonance frequencies of FSS layer. Figure 12 shows the reflection coefficient of FSS layer in this case for different values of inner and outer radii.

The two-layer FSS configuration made with two-sided square loop elements and their transmission coefficients versus frequency for different defect length are shown in Figure 13. The desired operating frequencies (defect modes) are located around the resonance frequencies of loops. Because of its small defect length, this configuration is extremely suitable for the design of multi-band low-profile high directive EBG antenna.

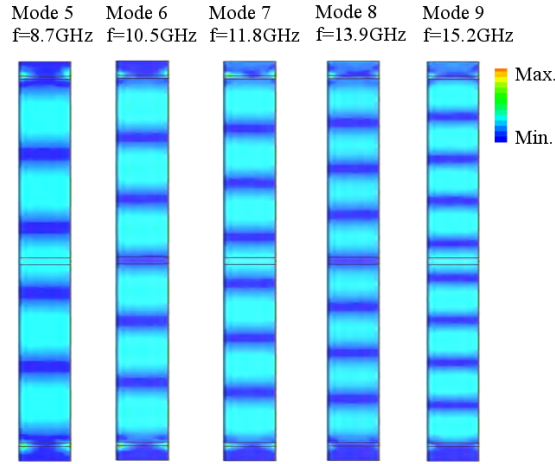


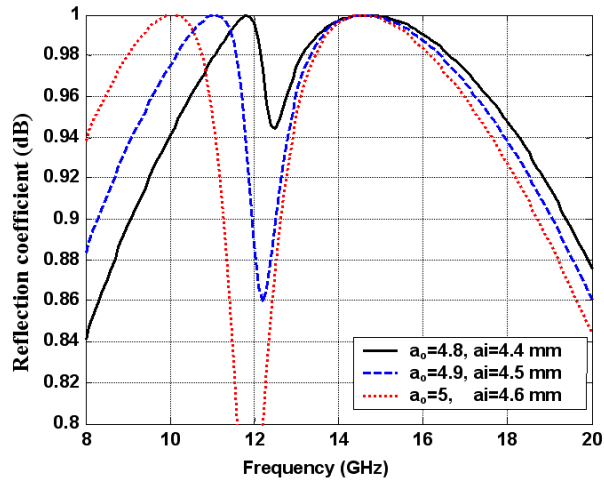
**Figure 11.** Electric field distribution of structure of Figure 10 for some important modes.

The bandgap of all configurations described in previous sections are represented in Table 1. It is seen that using more FSS layers create wider band gap. Also, FSS with double one-sided and two-sided elements have wide band gaps and can be used in designing low profile high directive antennas.

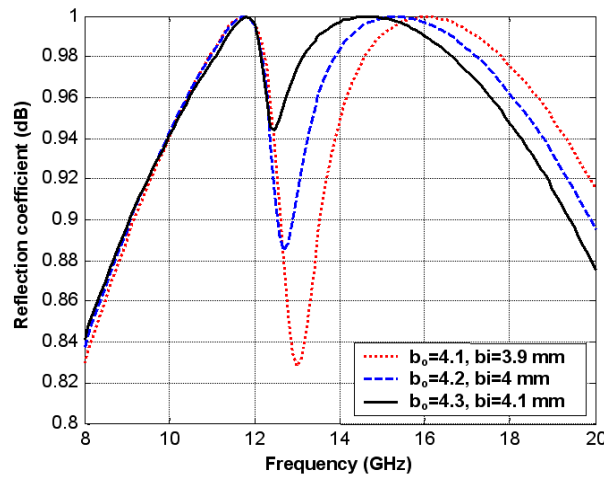
### 3. ANALYSIS OF THE WHOLE STRUCTURE

To confirm the results of the unit cell simulations, the radiation characteristics of patch antenna as primary radiation source in the presence of superstrate layer comprising of  $11 \times 11$  arrays is examined.

The single layer FSS superstrate configurations that offer appropriate gain and bandwidth have been examined in previous literatures [1, 2]. Also conventional method to achieve two operating frequency is using two superstrate layer. Disadvantage of this structure is that the effective height of this antenna increased twice regarding that of the antenna with one superstrate layer. To solve this problem we propose FSS with one (double) sided two square loop. But as mentioned in previous section one layer superstrate with one-sided two square loops have innate difficulties in manufacturing. Therefore, we propose the superstrate layer made by FSS layer with two-sided square loop. As was shown in previous section (Figures 13(a) and (b)) in this configuration without any limitation we can easily control the defect frequencies.



(a)



(b)

**Figure 12.** Reflection coefficients of the one-layer FSS with two-sided square loops versus frequency ( $P = 5.175$  mm) (a) for different  $a$  ( $b_o = 4.3, b_i = 4.1$  mm) (b) for different  $b$  ( $a_o = 4.8, a_i = 4.4$  mm).

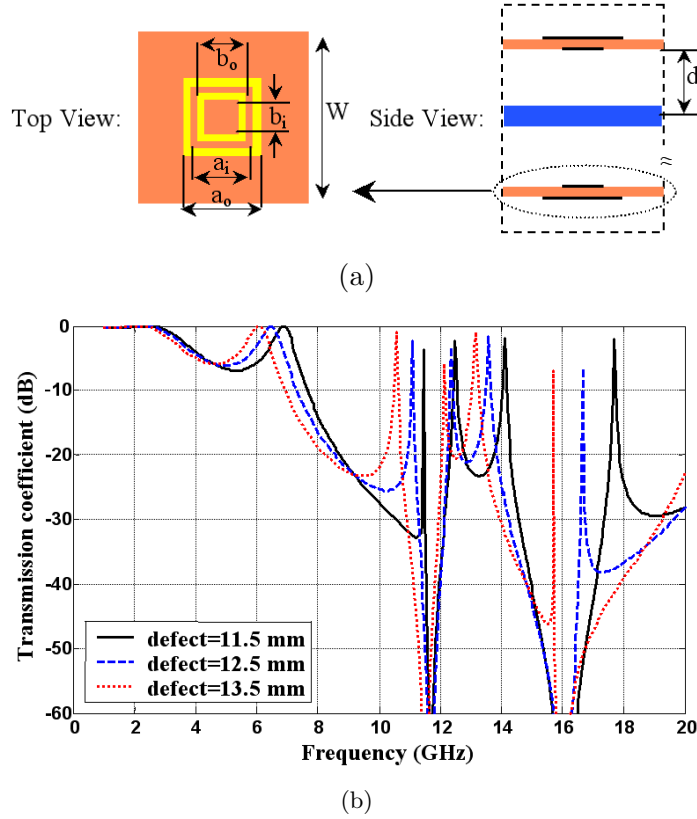


**Figure 13.** (a) Two-layer FSS with two-sided square loop elements (b) Its reflection coefficient versus frequency. ( $P = 5.175$ ,  $a - o = 4.8$ ,  $a_i = 4.4$ ,  $b_o = 4.1$ ,  $b_i = 3.9$  mm).

The antenna structure comprising superstrate layer and microstrip patch antenna as primary radiation source is depicted in Figure 14.

To obtain the maximum available power it is necessary to adjust the probe location of microstrip patch antenna for each frequency bands. Where is shown in Figure 15. As can be seen the optimum value of  $d_p$  (Probe Location) for first band is  $d_p = 2$  mm and for upper band is about  $d_p = 1.8$  mm.

Since the directivity of both bands are invariant with the variation of probe location, in final design we choose defect = 13.2 mm distance (Figure 13) between superstrate layer and ground plane. The final simulation results for lower and upper frequency bands are depicted in Figure 16.



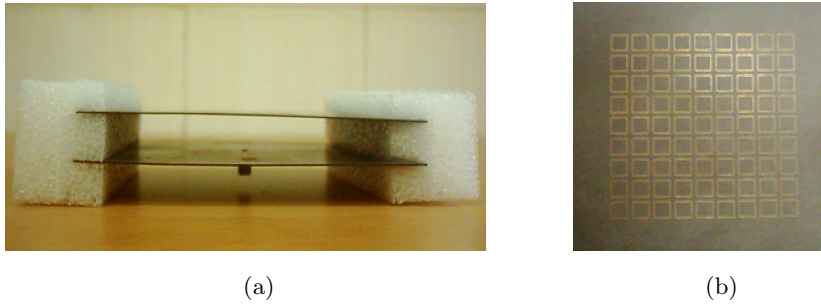


Figure 14. (a) Patch antenna with superstrate (b) Superstrate layer.

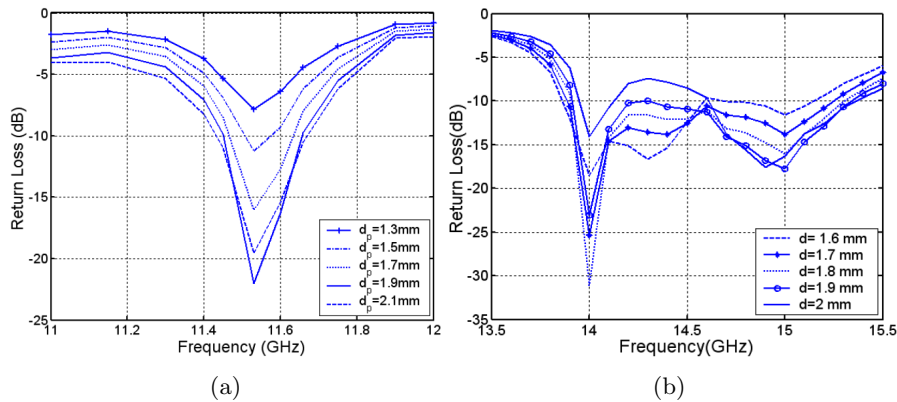


Figure 15. Effect of probe location on the return loss of antenna (a) lower band (b) upper band.

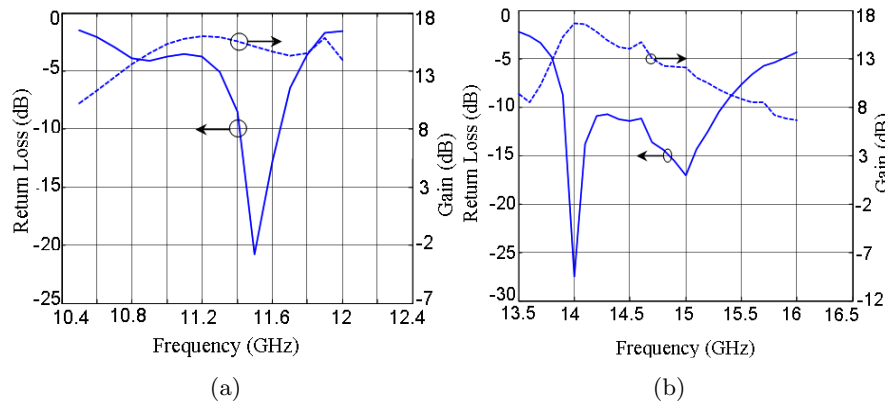
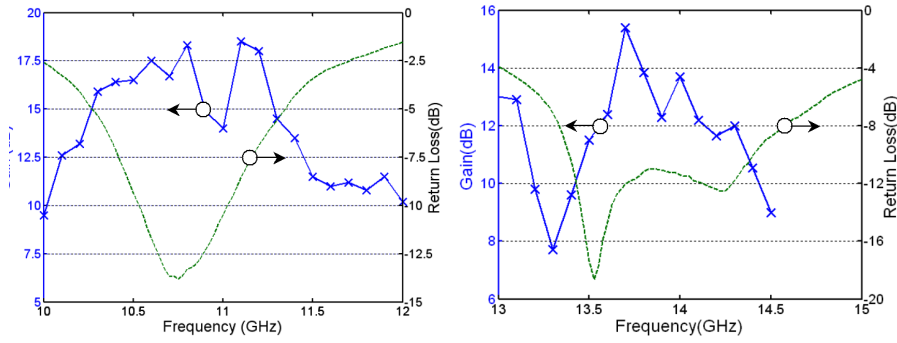
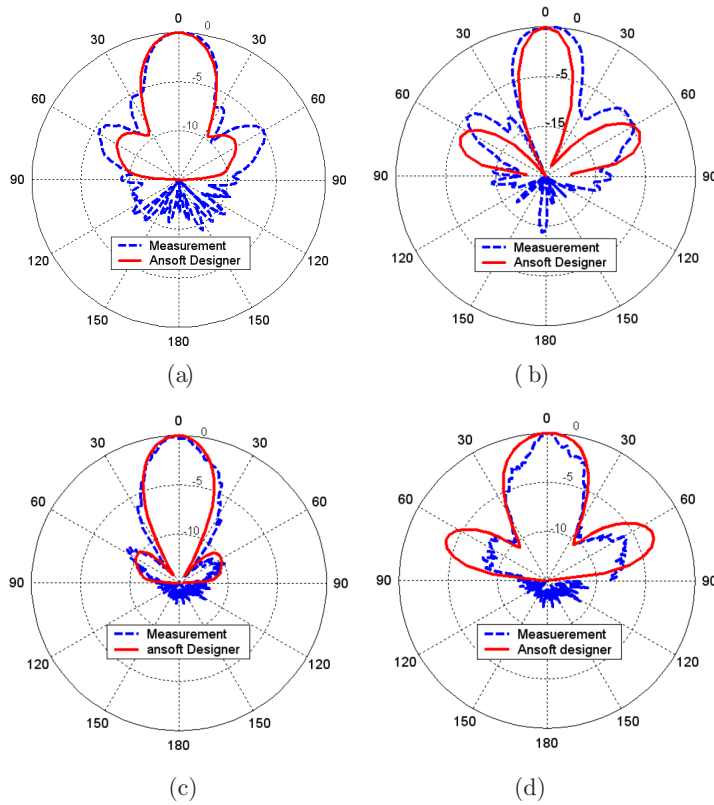


Figure 16. (a) RL and gain of antenna for lower band  $d_p = 2$  mm (b) RL and gain of antenna for upper band  $d_p = 1.8$  mm and ( $P = 5.175$ ,  $a_o = 4.8$ ,  $a_i = 4.4$ ,  $b_o = 4.1$ ,  $b_i = 3.9$  mm).



**Figure 17.** (a) Experimental results of RL and gain of antenna (a) lower band (b) upper band.



**Figure 18.** Radiation pattern of antenna (a)  $E$ -plane,  $f = 10.5$  GHz (b)  $H$ -plane,  $f = 10.5$  GHz (c)  $E$ -plane,  $f = 13.5$  GHz (d)  $H$ -plane,  $f = 13.5$  GHz.

Although the bandwidth of the first band at 11.5 GHz equals that of a simple probe fed patch antenna ( $\approx 3\%$ ), and the second band at 14 GHz shows a wider bandwidth ( $\approx 10\%$ ), the realized gains at both operating frequencies is about 15 dBi.

Also, experimental measurements of RL and Gain of antenna (Figure 17) for lower and upper frequency bands show good agreement with simulation results. Our mean of gain in all simulations is realized gain defined in Ansoft Designer software.

Figure 18 shows the radiation patterns at 10.5 GHz and 13.5 GHz for both the  $E$ - and  $H$ -planes.

#### 4. CONCLUSION

In this paper we first described the designing procedures of EBG antennas composed of a probe fed microstrip antenna and superstrate layer(s). Five different compositions of superstrate layers in a unit cell with periodic boundary conditions were simulated by means of the Ansoft Designer (Based on Method of Moment). After that, the most efficient structure, two-sided square loop FSS was selected as superstrate layer. The experimental and simulation results of the antenna reveal good agreements in return loss, realized gain, and radiation pattern. The results of this paper show that one can design an EBG antenna with square loop elements at any frequency.

#### ACKNOWLEDGMENT

The authors thank the Antenna Lab of the Iran Telecom Research Center (ITRC) and Microwave Lab of the Tarbiat Modares University for the support of this work.

#### REFERENCES

1. Pirhadi, A., M. Hakkak, and F. Keshmiri, "Bandwidth enhancement of the probe fed microstrip antenna using frequency selective surface as electromagnetic bandgap superstrate," *Progress In Electromagnetics Research*, PIER 61, 215–230, 2006.
2. Pirhadi, A., F. Keshmiri, and M. Hakkak, "Design of dual-band low profile high directive EBG resonator antenna, using single layer frequency selective surface superstrate," *IEEE APS/USNC/URSI Int. Symp.*, Albuquerque, New Mexico, USA, July 9–14, 2006.

3. Lee, Y. J., J. Yeo, R. Mittra, and W. S. Park, "Application of electromagnetic bandgap (EBG) superstrates with controllable defects for a class of patch antennas as spatial angular filters," *IEEE Trans. Antennas and Propag.*, Vol. AP-53, No. 1, 224–234, Jan. 2005.
4. Enoch, S., G. Tayeb, and B. Gralak, "The richness of the dispersion relation of electromagnetic bandgap materials," *IEEE Trans. Antennas and Propag.*, Vol. 51, No. 10, 2659–2666, October 2003.
5. Lee, Y. J., J. Yeo, K. D. Ko, and R. Mittra, Y. Lee, and W. S. Park, "A novel design technique for control of defect frequency of an electromagnetic band gap (EBG) superstrate for dual band directivity enhancement," *Microwave and Optical Technology Letters*, Vol. 42, No. 1, 25–31, July 2004.
6. Cheype, C., C. Serier, M. Thevenot, and T. Monediere, A. Reneix, and B. Jecko, "An electromagnetic bandgap resonator antenna," *IEEE Trans. Antennas Propag.*, Vol. 50, No. 9, 1285–1290, September 2002.
7. Lee, Y. J., J. Yeo, R. Mittra, and W. S. Park, "Design of a frequency selective surface (FSS) type superstrate for dual band directivity enhancement of microstrip patch antennas," *IEEE AP-S International Symposium and USNC/URSI National Radio Science Meeting*, Washington DC, July 2005.
8. Lee, Y. J., D. H. Lee, J. Yeo, W. S. Park, and R. Mittra, "Design of a frequency selective surface (FSS) superstrate with ring-shaped elements for directivity enhancement and low side lobe level of a circular polarization antenna," *International Symposium on Microwave and Optical Technology*, Vol. A-02, 11–14, Fukuoka, Japan, August 22–25, 2005.
9. Lee, Y. J., J. Yeo, R. Mittra, and W. S. Park, "Thin frequency selective surface (FSS) superstrate with different periodicities for dual-band directivity enhancement," *IEEE International Workshop on Antenna Technology: Small Antennas and Novel Metamaterial (IWAT)*, 375–378, March 2005.
10. Maagt, P. D., R. Gonzalo, Y. C. Vardaxoglou, and J. M. Baracco, "Electromagnetic bandgap antennas and components for microwave and (sub) millimeter wave application," *IEEE Trans. Antennas and Propag.*, Vol. 51, No. 10, 2667–2677, 2003.
11. Lee, Y. J., J. Yeo, R. Mittra, and W. S. Park, "Design of high-directivity electromagnetic band gap (EBG) resonator antenna using a frequency selective surface (FSS) superstrate," *Microwave and Optical Technology Letters*, Vol. 43, No. 6, 462–467, 2004.